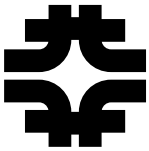

Fermi National Accelerator Laboratory

FERMILAB-FN-689

Fermilab Electron Cooling Project: Estimates for the Cooling Section Solenoid

S. Nagaitsev and A. Shemyakin

Fermi National Accelerator Laboratory
P.O. Box 500, Batavia, Illinois 60510

V. Vostrikov

Budker INP
Novosibirsk, Russia

March 2000

Operated by Universities Research Association Inc. under Contract No. DE-AC02-76CH03000 with the United States Department of Energy

Fermilab Electron Cooling Project: Estimates for the Cooling Section Solenoid

S. Nagaitsev, A. Shemyakin, Fermilab, USA
V. Vostrikov, Budker INP, Novosibirsk, Russia

1. Introduction

A final goal of the Electron Cooling R&D efforts at Wide Band building is a round electron beam with a kinetic energy of 4.3 MeV propagating through a cooling section with transverse angles below $1 \cdot 10^{-4}$ rad [1]. The latter requirement is important because electrons with angles above this critical value have a reduced cooling ability. Electron angles in the cooling section largely depend on the magnetic field quality. The goal of this work is to analyze possible perturbations of the magnet field and their influence on electron motion. Such an analysis must be done to choose the solenoid design and the winding technology.

The proposed cooling section consists of ten modules equipped with identical solenoids. Some parameters of a solenoid module are shown in Table 1.

Table 1: The basic parameters of the cooling section solenoids.

Parameter	Symbol	Value	Units
Solenoid length	l_s	190 - 196	cm
Solenoid ID	$2a$	15	cm
Magnetic field	B_0	50 - 150	G

Neighboring solenoids are divided by a gap where a vacuum pump port, scrapers, and BPM feedthroughs are placed. Effects of magnetic field perturbation because of gaps and because of winding errors in the homogeneous part of solenoids are considered separately in Sections 2 and 3, respectively.

The consideration is limited to a case of an initially “cold” electron beam in which all electrons enter the cooling section parallel to its axis. This model can be used because all perturbation effects must be small and, therefore, linear expansions are valid. The linearity gives also a possibility to discuss separately different sorts of perturbation.

In this paper, we assume that an angle acquired by an electron because of passing through a specific perturbation has to be below $2 \cdot 10^{-5}$ rad while an angle inside a perturbed region should be kept under $7 \cdot 10^{-5}$ rad. In this case, full electron angles might be under boundary of ineffective cooling ($1 \cdot 10^{-4}$ rad).

All estimations were done for the magnetic field strength of 150 G and the initial electron radius of 5 mm. Gaussian units are used. Numerical simulations of magnetic fields and single particle motion were done by the computer code SAM 3-0 [2].

2. Effects of a gap

2.1 General consideration

First, we consider the effects of longitudinal field variations caused by a gap between solenoids.

The electron Larmor oscillation period in the cooling section is 6.3 – 20 m while the gap size is much smaller (6 – 10 cm). Typical magnetic field distribution along the z-axis is shown for a gap in Fig. 1. In this case, the gap between solenoids generates an angular perturbation similar to a thin lens. A radial angle $\delta r'_{out}$ acquired while traversing the gap can be found from the equation of the particle motion in an axially symmetric magnetic field [3]:

$$\frac{d^2 r}{dz^2} - \left[\frac{r_0^4}{r^4} - \frac{B^2(z)}{B_0^2}\right] \cdot \frac{r}{4\rho_L^2} = 0 \ , \tag{1}$$

where $\rho_L = \gamma\beta mc^2/eB_0$ is the Larmor radius, γ and $\beta = v/c$ are the usual Lorentz factors, $B(z)$ and B_0 are magnetic fields inside the gap and in the homogeneous part of the solenoid, respectively.

In a case of a paraxial motion and a thin lens approximation ($r \approx r_0$ inside the gap), the acquired angle is

$$\delta r'_{out} = \frac{r}{4\rho_L^2} \cdot \int_{gap} \left(1 - \frac{B^2(z)}{B_0^2}\right) dz \ . \tag{2}$$

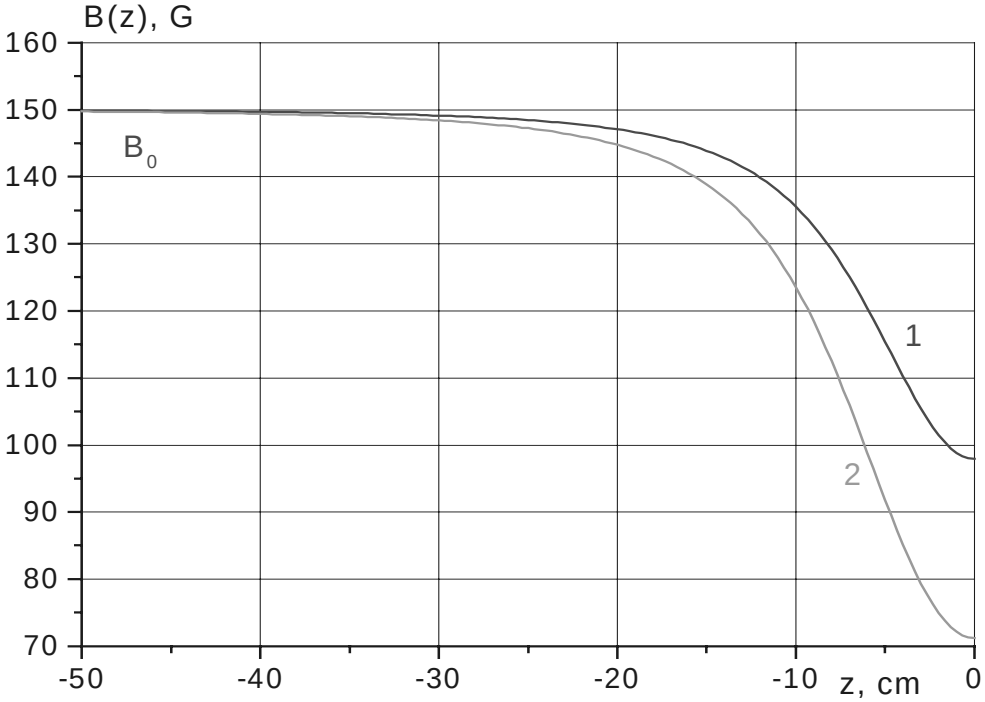

Figure 1: The longitudinal field on-axis in a gap between two semi-infinite solenoids as a function of z coordinate. Curves 1 and 2 show results for 6 and 10 cm gaps, respectively.

After passing through the gap an electron begins to spiral so that the total transverse velocity is constant. Fig. 2 shows the total electron angle, given by

$$\theta_t = \sqrt{\left(\frac{v_r}{\beta c}\right)^2 + \left(\frac{v_\theta}{\beta c}\right)^2}\,, \tag{3}$$

along the trajectory for the case of 6 and 10 cm gaps. Two separate effects can be distinguished.

First of all, after passing the gap region, an electron has an angle θ_{out} more than the critical value. To correct the angle, one can add short solenoids (correctors) near the gap so that

$$\int_{gap}\left(1-\frac{B^2(z)}{B_0^2}\right)dz = 0\,, \tag{4}$$

and the total angle is zero inside the next downstream part of the main solenoid. The angle is precisely compensated for one trajectory; a residual transverse motion of electrons persists at other radii because of non-linear field components.

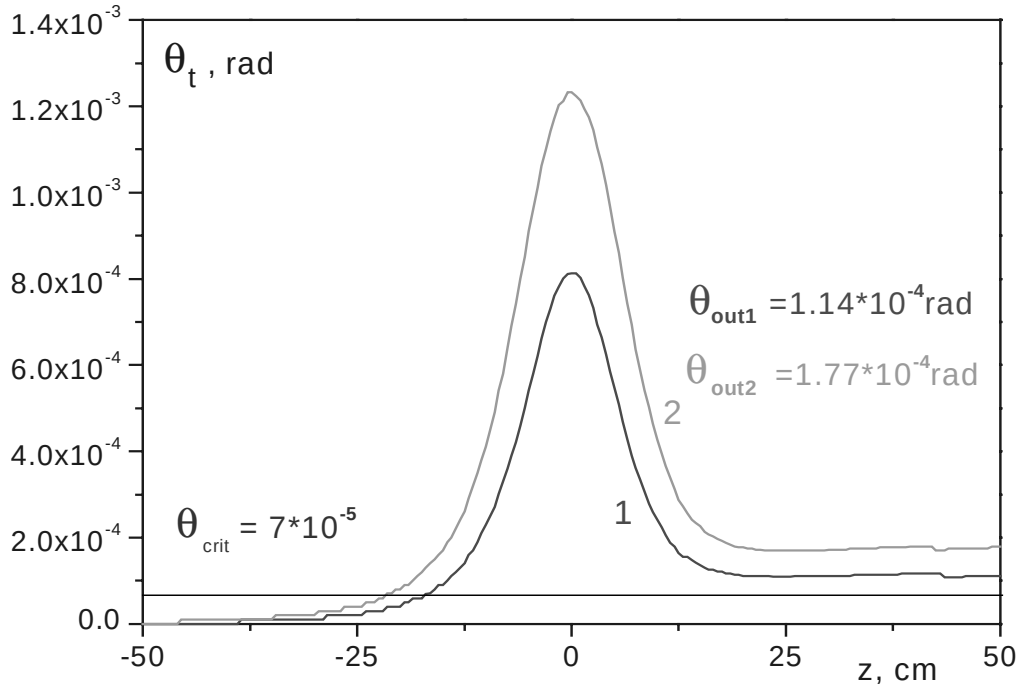

Figure 2: The total angle acquired in the gap by an electron at r = 5 mm. Curves 1 and 2 show results for 6 and 10 cm gaps, respectively. The solid line indicates the critical angle of 7×10^{-5} rad.

Let us estimate a restriction on the corrector currents due to condition (4). The gap is equivalent to a superposition of a homogenous solenoid and a short solenoid with a length equal to the gap size δ and the current of $(-j_0\cdot\delta)$, where j_0 is the linear solenoid

current density (in Amp·turns/cm). The field perturbation is a sum of this short solenoid field B_1 and the corrector fields B_i

$$\Delta B(z) = B(z) - B_0 = B_1 + \sum_i B_i \,. \tag{5}$$

Note, that

$$\int_{gap} \left(B_1 + \sum_i B_i \right) dz \approx \int_{-\infty}^{+\infty} \left(B_1 + \sum_i B_i \right) dz = \frac{4\pi}{c} \cdot \left(\sum_i I_i - j_0 \delta \right), \tag{6}$$

where I_i are the currents of the correctors. Taking into account eq. (6), condition (4) can be rewritten as follows:

$$\frac{4\pi}{c} \cdot \left(\sum_i I_i - j_0 \delta \right) = \frac{B_0}{2} \cdot \int_{gap} \left(\frac{\Delta B(z)}{B_0} \right)^2 dz = \frac{2\pi}{c} \cdot j_0 \delta \cdot \left(\frac{\langle \Delta B \rangle}{B_0} \right)^2 . \tag{7}$$

Here <ΔB> is a rms. value of the field perturbation over the gap. Eq. (7) gives us the restriction for corrector currents

$$\sum_i I_i = j_0 \cdot \delta \cdot \left(1 - \frac{1}{2} \cdot \left(\frac{\langle \Delta B \rangle}{B_0} \right)^2 \right). \tag{8}$$

In the practically interesting case of a low field perturbation, $\langle \Delta B \rangle << B_0$,

$$\sum_i I_i = j_0 \cdot \delta \tag{9}$$

with a precision sufficient for our purpose. The meaning of eq. (9) is quite simple. To have no focusing effects in the gap in the first order, it is enough to keep average density of Ampere-turns in the gap equal to that of the regular part of the solenoid.

The second harmful effect of a gap is an azimuthal angle, θ_φ, which electrons have inside the gap. If $\Delta B << B_0$,

$$\theta_\varphi = \frac{r}{2\rho_L} \cdot \frac{\Delta B}{B_0} \,. \tag{10}$$

The restrictions for these two angles (θ_φ and θ_{out}) vary. The remaining total angle, θ_{out}, contributes to a motion downstream of the gap and has to be lower than $2 \cdot 10^{-5}$ rad. The angle θ_φ exists inside the perturbed region only and disappears when $B \to B_0$. It can not be set to zero in the gap, and the critical value of $7 \cdot 10^{-5}$ rad determines the length, L_g, of a region around the gap where the cooling is ineffective because of large azimuthal velocities.

Two possible solutions for decreasing both the angles after passing the gap, θ_{out}, and the length, L_g, of the region where cooling is ineffective were considered. Namely, (1) two pairs of correction coils without a magnetic shield and (2) one pair of coils with a shield. These variants were simulated numerically. In the simulations, electron started from the middle of a 2 m solenoid at radius of 5 mm parallel to the axis, and tracking was stopped inside the next module when the angle θ_t became constant ($\theta_t = \theta_{out}$). All simulations were done for $B_0 = 150$ G.

2.2 Two pairs of correction coils

The first set of simulations was done for a case of solenoids without any magnetic shielding. To correct the field perturbation, two solenoidal coils were placed on both sides of the gap. The results of simulations are similar for various coil locations: inside the main solenoid, outside of it or made as part of the main solenoid (see Fig.3). The geometry is symmetric with respect to the central plane of the gap.

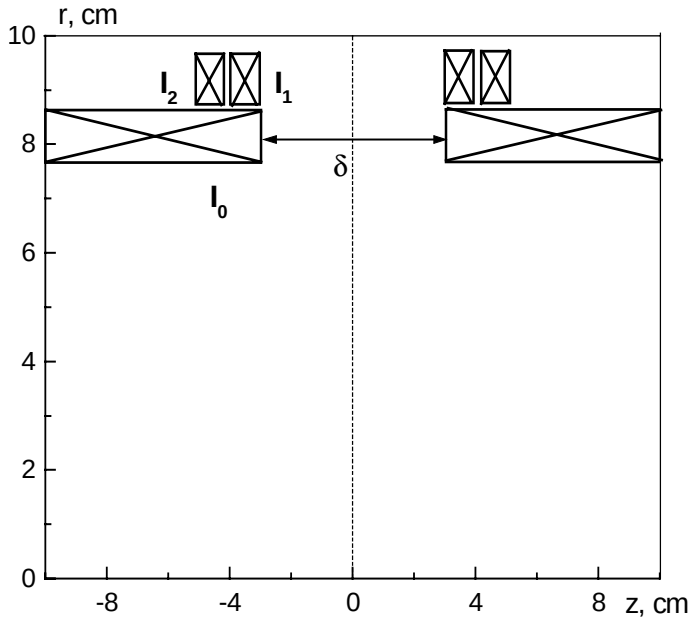

Figure 3: The geometry of the gap with two pairs of correction coils.

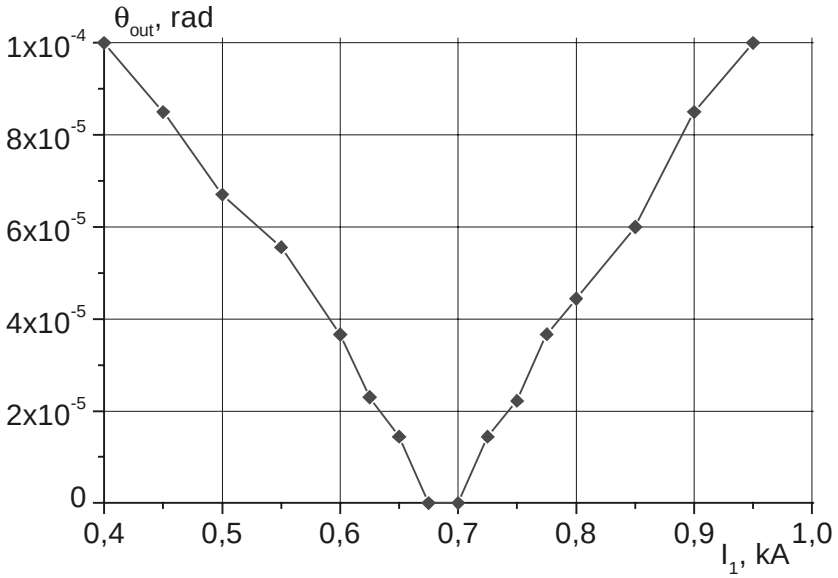

Figure 4: The total angle θ_{out} after passing a 6 cm gap as a function of current in inner coils. The current in each of outer coils is –0.32 kA.

The current direction in coils nearest to the gap is the same as in the main solenoid. The coils increase the magnetic field strength inside the gap. The second pair of coils has an opposite sign of current. These coils decrease a field maximum under the first correction coils.

Fig. 4 shows the total angle θ_{out} as a function of current in the inner coils at a constant current in the second pair of correction coils. Values of currents corresponding to a zero θ_{out} are in good agreement with equation (9).

The curve in Fig.4 was calculated for an electron at a 5 mm radius. Angles acquired by electrons at different radii are shown in Fig.5 for the corrector currents that correspond to $\theta_{out} = 0$ at r = 5 mm. These angles are determined by spherical aberration, and the curve fits a cubic function,

$$\theta_{out} = C_s r^3 \tag{11}$$

with C_s being $3.1 \cdot 10^{-7}$ cm^{-3}. The aberrations are lower than the precision of the simulation at r<10 mm and are negligible for our purposes.

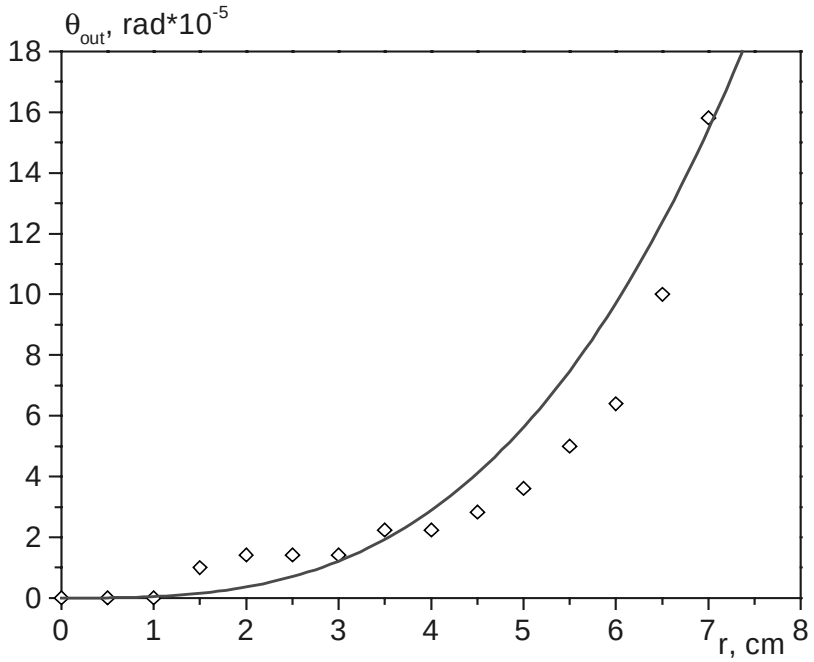

Figure 5: The total angle θ_{out} after passing a 10 cm gap as a function of the electron radius. Currents in the correctors are 2.5 and -1.9 kA.

The next step is to minimize the length L_g of a region around the gap where the cooling is ineffective because of large azimuth velocities (>$7 \cdot 10^{-5}$ rad at the 5 mm radius). Fig. 6 shows the length L_g as a function of the inner coil current. Note that the simulation was done for the case of θ_{out}=0, and the current in the second pair of coils was calculated from equation (9). Fig. 7 shows absolute values of the azimuthal angle for the case of optimum corrections. The angles were found to be below $7 \cdot 10^{-5}$ rad over all the gap at optimum correction currents so that L_g =0 (See Fig. 8.). Corresponding field distribution along the axis is presented at Fig. 9. These results are summarized in Table 2.

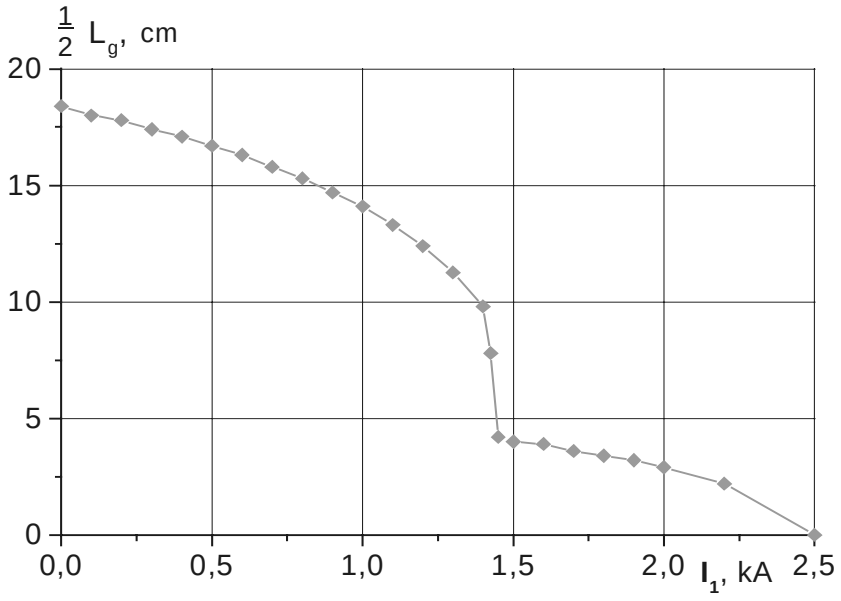

Figure 6: The length L_g as a function of the current in the inner coil while $\theta_{out}=0$. The gap size is 10 cm .

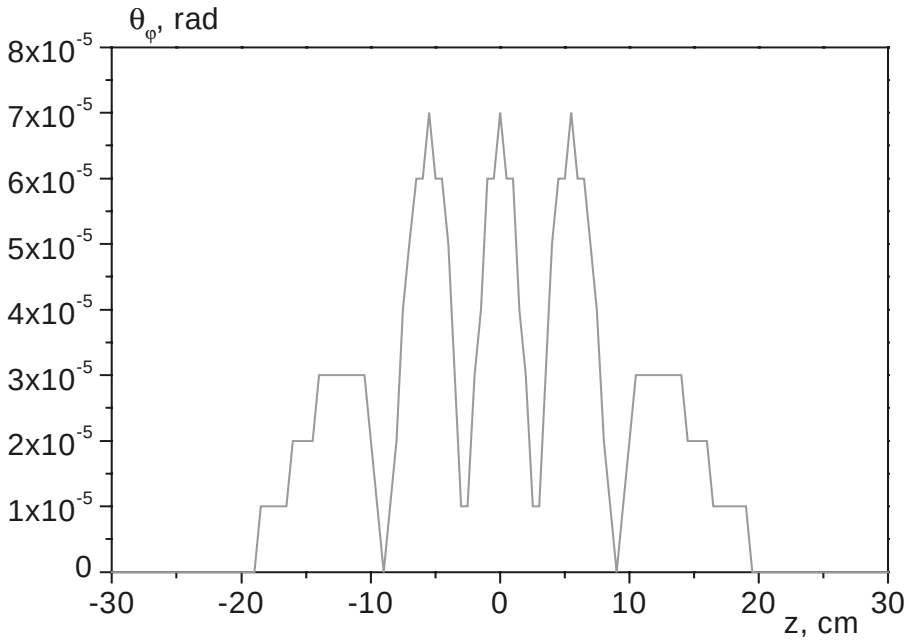

Figure 7: The azimuthal angle (absolute value) as a function of the longitudinal coordinate. Gap size is 10 cm, currents of correctors are I_1 = 2.5 and I_2 = – 1.9 kA.

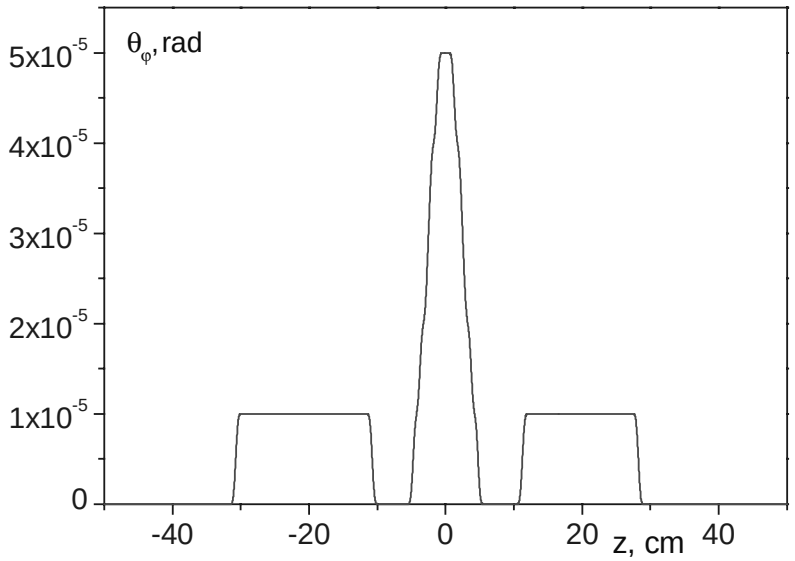

Figure 8: The azimuthal angle (absolute value) as a function of the longitudinal coordinate. Gap size is 6 cm; currents of correctors are 1.04 and –0.69 kA.

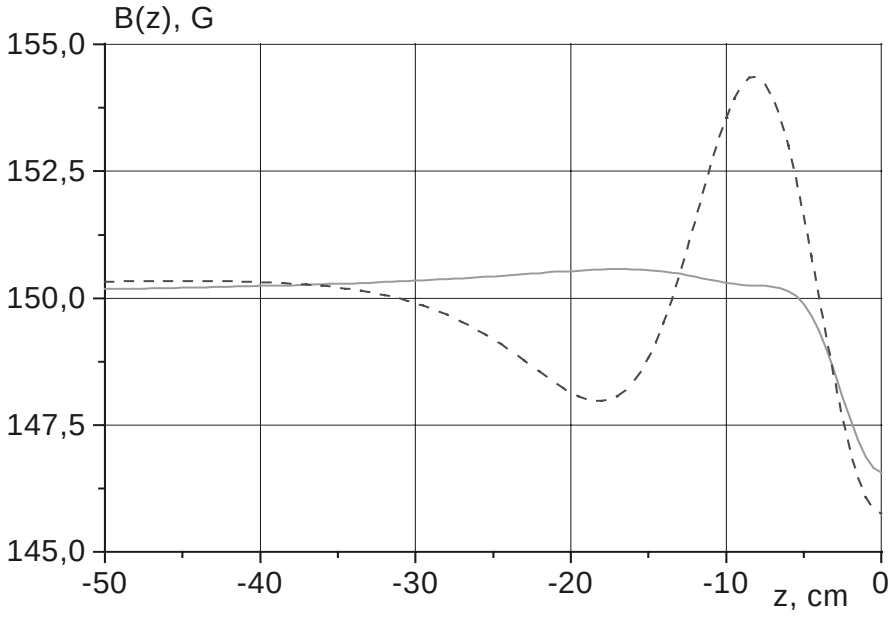

Figure 9: The longitudinal magnetic field as a function of z-coordinate for the case of optimum corrections (see Table 2). Solid and dash curves correspond to 6 and 10 cm gaps sizes, respectively.

Table 2: The optimum settings of correctors. The setting #2 is a compromise between the perturbation length and a value of corrector currents.

Setting #	Gap size δ, cm	Current in inner coil, kA	Current in outer coil, kA	Length of perturbation L_q, cm
1	6	1.04	-0.68	0
2	10	1.5	-0.9	8
3	10	2.5	-1.9	0

2.3 Pair of correction coils with a magnetic shield

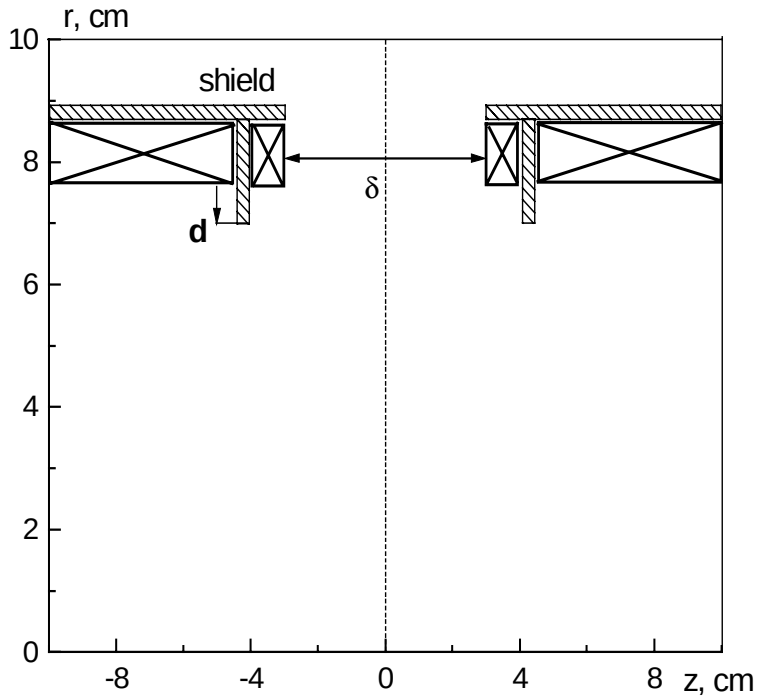

Figure 10: The simulated geometry of the gap effect compensation by a pair of coils and a magnetic shield.

The design discussed above needs an adjustment of two pairs of coils and a comparatively high value of their currents. A simplification can be made by a use of a magnetic shield protruding inside of the solenoid (Fig. 10). In this case, the coil currents

have to satisfy the equation (9) while the length d of the shield protrusion is the parameter which can be varied to optimize the length L_g of the ineffective cooling region.

Simulations similar to those described in the previous section were performed. Results for two gap sizes are presented in Table 3. The permeability of the magnetic shield was taken to be equal to 1000. Figures 11 and 12 show the field and angle distributions along the z-coordinate. The minimum perturbation length, L_g, is 8 cm for the 10 cm gap, which is still much less than the full length of the module (2 m).

Table 3: The length of perturbation for optimum parameters of the design with a shield

Gap size δ, cm	Coil current, kA	Protrusion length d, mm	Length of perturbation L_g, cm
6	0.604	0	~1
10	0.865	5	8

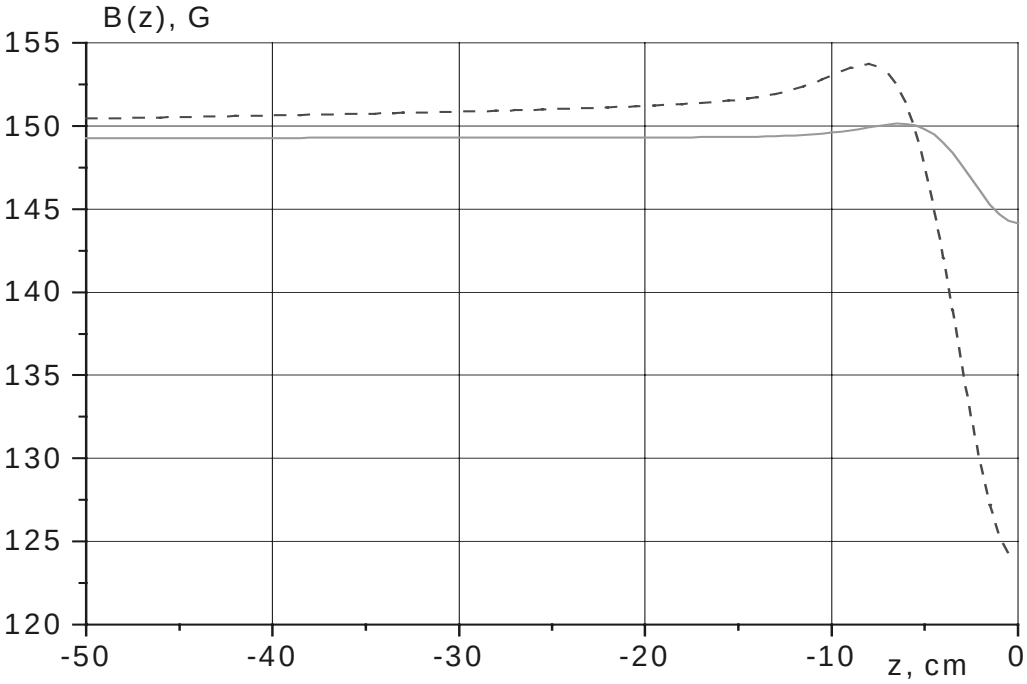

Figure 11: The longitudinal magnetic field as a function of z coordinate. The solid and dash curves correspond to the 6 and 10 cm gaps respectively.

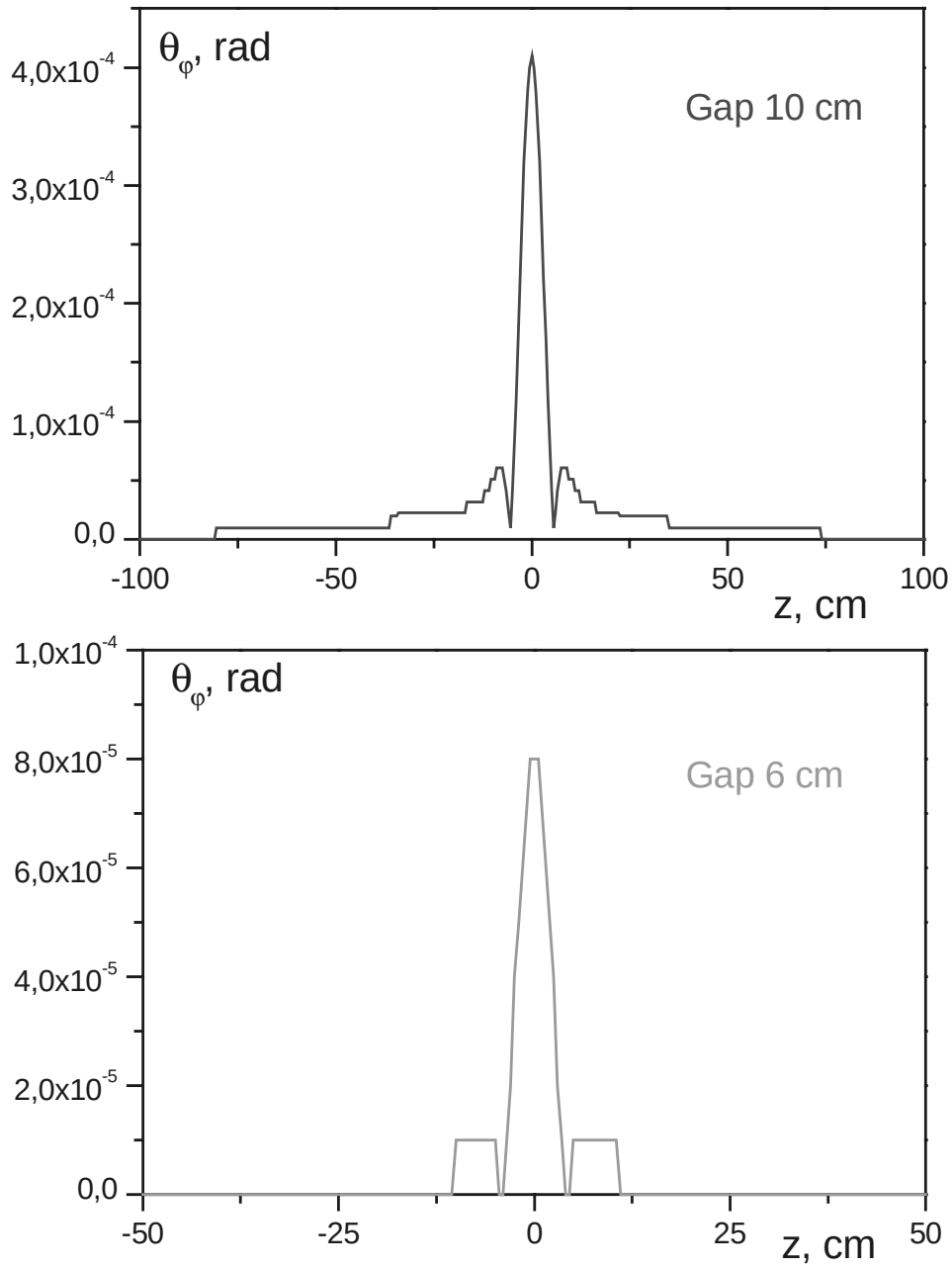

Figure 12: The azimuthal angle in the gaps (absolute value) with the optimum adjustment of magnetic shield geometry and the correction coil currents.

3. Magnetic field perturbations inside the solenoid

3.1 Single-coil solenoid design

The solenoid can be manufactured as a single coil (Fig.13). Some of its parameters are listed in Table 4.

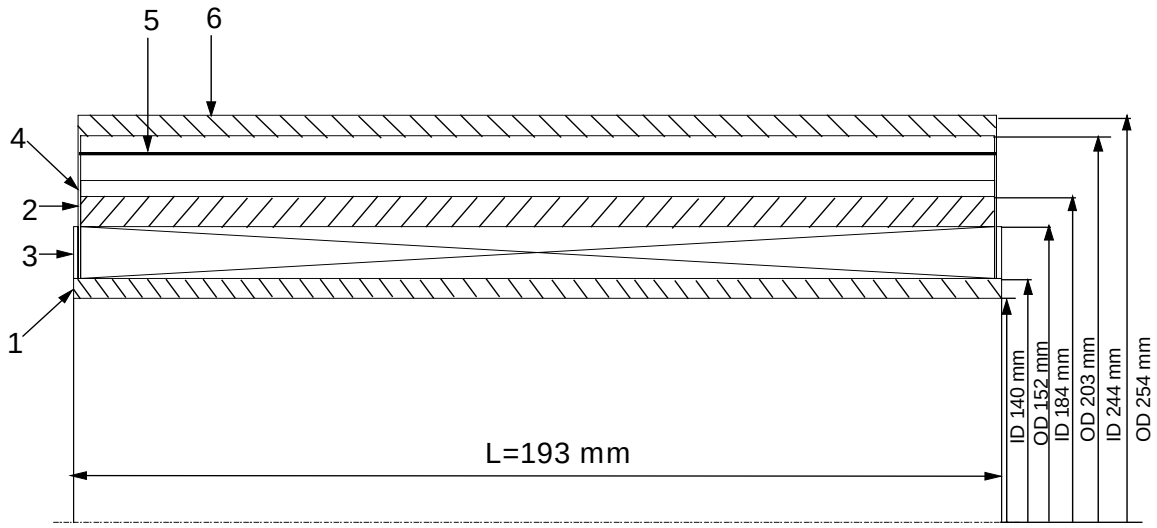

Figure 13: The cooling section solenoid module. 1- inner aluminum tube, 2- outer aluminum tube, 3- gap correctors, 4- dipole correctors layer, 5- μ-metal shield, and 6- iron magnetic shield.

Table 4: Proposed parameters of the module solenoid.

Number of layers	6
Number of turns in one layer	1000
Wire diameter	2 mm
Current for B=150 G	4 A
Total weight	250 kg
Power	240 W

It is proposed to wind the solenoid around a 6” OD aluminum tube with a 2- mm diameter copper wire. The low wire diameter helps to maintain a good precision of winding; moreover, an increased number of turns averages out field errors caused by deviations of wire positions from an ideal spiral. The chosen wire size is a compromise

which gives an acceptable total voltage drop over ten solenoids connected in series. We prefer to make an even number of layers to avoid problems with a current return path.

The main parameter determining solenoid quality is the magnitude of transverse components of the magnetic field. An electron propagating through a short region with a dipole field $B_\perp$ acquires an angle θ_d:

$$\theta_d = \frac{1}{B_0 \rho_l} \cdot \int B_\perp dz \,. \tag{12}$$

The shortest scale of dipole field variations is the solenoid diameter, which is much larger than the beam size. Therefore, the field effects are nearly identical for all electrons in the beam, and we can consider only the motion of an electron entering the solenoid on axis.

The restriction to such perturbations is the same as was discussed in Section 1, namely, an electron angle should never exceed $7 \cdot 10^{-5}$ rad. For an electron with kinetic energy of 4.3 MeV, this angle corresponds to an integral of the dipole field of 1 G·cm. All perturbations exceeding this level should be corrected by dipole coils placed over the solenoid body. Note that this scheme assumes that angles at the entrance and exit of every module are low. Analogously to Section 2, the limit for the angles is taken equal to $2 \cdot 10^{-5}$ rad.

A dipole field of any realistic distribution can be compensated by a system of dipole correctors. The main questions for this section are: (1) what is the minimum number of the correctors and (2) how strong they have to be for practically achievable tolerances of solenoid manufacturing?

One of the dangerous perturbations for the future electron cooling device is a time-dependent dipole field from the Main Injector current buses. A typical size of the fringe fields is several meters. To preserve electron angles, resulting from these fields, under $2 \cdot 10^{-5}$ rad, the cooling section should be magnetically shielded with restriction for a residual field value of about 1 mG. We intend to use a two-layer magnetic shield: a thin inner soft-iron layer and a thicker outer magnetic steel tube, which works also as a flux return. Detailed calculations and the shield design are still ahead and will not be considered in this paper.

Below we discuss ways to correct solenoid misalignments, mechanical distortions of the solenoid body, and winding errors.

3.2 Perturbations because of misalignments

Suppose that all module solenoids but one are well aligned with respect to an axis and an electron beam propagates along that same axis. The considered solenoid can be inclined and shifted.

In the paraxial approximation, the transverse magnetic field components $\vec{B}_{\perp 1}$ near the entrance of a solenoid are proportional to the distance $\vec{r}_1$ from its axis. The fields of the solenoid, shifted by Δ, can be presented as a sum of fields of a well-aligned solenoid, $\vec{B}_{\perp 0}$, and a dipole:

$$\vec{B}_{\perp 1} = k \cdot \vec{r}_1 = k \cdot (\vec{r} + \vec{\Delta}) = \vec{B}_{\perp 0} + k \cdot \vec{\Delta}, \tag{13}$$

where $k = -\frac{1}{2}\frac{dB_z}{dz}$. The angle θ_Δ, which an on-axis electron acquires in this case, is equal to the one appearing if a non-magnetized electron shifted from the axis by Δ enters an aligned solenoid:

$$\theta_\Delta = \frac{\Delta}{2\rho_L}. \tag{14}$$

To avoid this effect (i.e. $\theta_\Delta < 2\cdot10^{-5}$ rad), solenoids should be aligned to within 0.02 mm.

The inclination of a solenoid by an angle α_i also induces a transverse component equal to $\alpha_i \cdot B_0$. The resulting electron angle is less than $2\cdot10^{-5}$ rad, if $\alpha_i \cdot < 1\cdot10^{-5}$ rad.

Both restrictions seem to be severe for mechanical alignment, but can be satisfied with the use of correction dipole coils. An inclination can be corrected by a pair of X and Y coils placed along the whole solenoid, and short coils near the solenoid exit can correct a shift of axes. The question of how to measure these misalignments with a necessary precision is very important, but it is outside the scope of this paper.

3.3 Mechanical distortion

The solenoid body can be distorted because of its weight and length. Supporting the body with a precision of tens micrometers during winding seems to be too expensive in comparison with adding dipole correctors. To estimate how strong these effects could be, let us consider an extreme case: the whole weight of the solenoid module wound on a 6" OD, 5.5" ID aluminum tube is supported in two points at its ends. For parameters listed in Table 4, the sag t in the middle is about 0.4 mm. Suppose, that the bend is parabolic and the magnetic field follows the curved mechanical axis. Then the resulting vertical magnetic field is linear with the axial coordinate z:

$$B_y(z) = B_{\perp\max} \cdot \frac{2z - l_s}{l_s}\ , \tag{13}$$

where $B_{\perp\max} = \frac{4t}{l_s} \cdot B_0 = 0.12$ G, l_s = 200 cm is the solenoid length, and z is counted from the end of the solenoid. The integral of B_y over the solenoid is equal to zero; however, the electron angle in the middle of the solenoid, θ_{mid}, is about $4.2\cdot10^{-4}$ rad.

We can place dipole correctors evenly along the solenoid and adjust their fields B_{cor} so that the resulting transverse field in the middle of every corrector $(B_y + B_{cor})$ is zero. Because of the linearity of $B_y(z)$, the angle is canceled at the end of correctors and has the maximum, θ_{cor}, in the center of a corrector:

$$\theta_{cor} = \frac{\int_0^{L/2} (B_y + B_{cor})\, dz_1}{B_0\rho_L} = \frac{B_{\perp\max}}{B_0\rho_L} \cdot \left(\frac{L}{2l_s}\right)^2 = \frac{\theta_{\mathrm{mid}}}{N_{cor}^{\ 2}}\ , \tag{14}$$

where z_1 is counted from a corrector edge, L is a corrector length, and $N_{cor} = \frac{l_s}{L}$ is a number of correctors. Obviously, the total number of correctors has to be even. For

$N_{cor}=4$, the angle θ_{cor} = $2.6\cdot10^{-5}$ rad. Therefore, four pairs of correctors seem to be sufficient to correct mechanical distortion of the solenoid body.

3.4 Winding errors.

Winding errors, or deviations of winding from an ideal spiral, seem to be the most fundamental factor determining the solenoid field quality. We will estimate the effects of winding errors in the framework of a model where the solenoid is represented by a set of identical thin closed-loop coils with current equal to the solenoid current. The radius of the coils is equal to the average solenoid radius, and the number of coils is the same as the total number of turns in the solenoid. The ideal winding corresponds to coaxial coils evenly distributed along the solenoid length.

Three types of errors are considered below: random shifts of coils in the transverse direction, their random tilt, and a non-uniformity of the coil distribution along the solenoid.

The paraxial approximation of the magnetic field of a separate unperturbed coil is

$$B_z = B_c \cdot \frac{1}{\left(1+\frac{z^2}{a^2}\right)^{\frac{3}{2}}}, \quad B_r = \frac{3B_c}{2a^2}\cdot\frac{zr}{\left(1+\frac{z^2}{a^2}\right)^{\frac{5}{2}}}, \quad B_c = \frac{2\pi I}{a\cdot c}, \tag{16}$$

where z is counted from the coil center, a is a radius of the coil, and I is the coil current [4]. If one coil is shifted in the x direction by δx, an x- component of the field $(\tilde{B}_x)_{shift}$ appears on the axis, such that

$$(\tilde{B}_x)_{shift} = B_c \cdot \frac{3}{2a^2}\cdot\frac{z\cdot\delta x}{\left(1+\frac{z^2}{a^2}\right)^{\frac{5}{2}}}. \tag{17}$$

The angle, θ_{shift_0}, of an electron trajectory arising from this shift has a maximum in the center of the coil,

$$|\theta_{shift\_0}| \approx \frac{\left|\int_{-\infty}^{0}(\tilde{B}_x)_{shift}\,dz\right|}{B_0\rho_L} = \frac{B_c}{B_0}\cdot\frac{\delta x}{2\rho_L} = \frac{\delta x}{2\rho_L}\cdot\frac{1}{N_{eff}}, \tag{18}$$

where N_{eff} is the number of turns on the length equal to the solenoid diameter $2a$. The resulting angle after passing through such a coil becomes much less than θ_{shift_0} at $z> a$ so that the total angle because of all randomly shifted coils θ_{shift} is about $\sqrt{N_{eff}}$ times larger:

$$\theta_{shift} \approx \theta_{shift\_0}\cdot\sqrt{N_{eff}} \approx \frac{\delta x}{2\rho_L}\cdot\frac{1}{\sqrt{N_{eff}}}. \tag{19}$$

The calculation is similar for the case of randomly tilted coils. The x- component of the field of a coil tilted by α in the xz-plane is

$$(\tilde{B}_x)_{tilt} = B_z \cdot \sin\alpha + B_r \cdot \cos\alpha = B_c \cdot \frac{1+\frac{3}{2}\cdot\frac{z^2}{a^2+z^2}}{(1+\frac{z^2}{a^2})^{\frac{3}{2}}} \cdot \sin\alpha\,, \tag{20}$$

where z is in non-rotated coordinates. The angle after passing through the coil is

$$\theta_{tilt\_0} \approx \frac{\int_{-\infty}^{\infty}(\tilde{B}_x)_{tilt}\,dz}{B_0\rho_L} = \frac{B_c}{B_0}\cdot\frac{\delta x}{2\rho_L} = \frac{2a\cdot\sin\alpha}{\rho_L}\cdot\frac{1}{N_{eff}} = \frac{\Delta}{\rho_L}\cdot\frac{1}{N_{eff}}\,, \tag{21}$$

where Δ is the relative shift of coil ends. The result for the case of all coils tilted by an angle α with a random sign is higher by about the square root of the total number of coils in the solenoid, which is $(N_{eff}\cdot\frac{l_s}{2a})$:

$$\theta_{tilt} \approx \frac{\Delta}{\rho_L}\cdot\frac{1}{\sqrt{N_{eff}}}\cdot\sqrt{\frac{l_s}{2a}}\,. \tag{22}$$

This angle exceeds the one caused by shifts (see (19)) by a factor of $2\cdot\sqrt{\frac{l_s}{2a}} \approx 7$ for the same precision of winding.

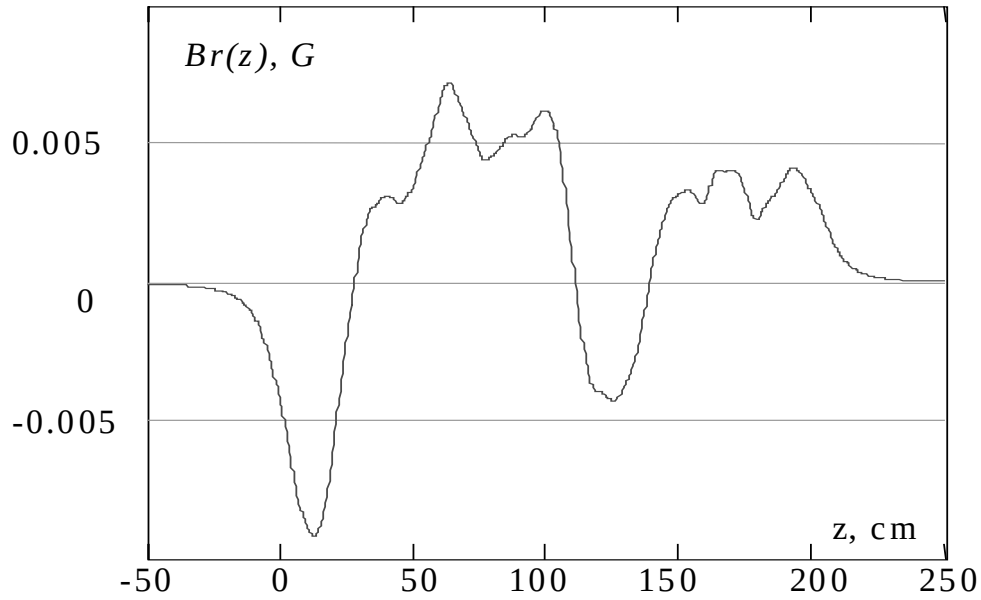

Figure 14: A typical behavior of the transverse magnetic field along the longitudinal coordinate. The simulation was done for 6000 coils of 15 cm diameter, evenly distributed from 0 to 200cm. The coils are randomly inclined by angles having a Gaussian distribution with a standard deviation of $\alpha_0 = 5\cdot10^{-4}$ rad. The longitudinal magnetic field is 150 G.

The effect of tilted coils was also examined by a computer simulation for parameters listed in Table 4. The coil incline angles had a random Gaussian distribution

with a standard deviation α_0 and the transverse field was calculated by the formula (20). The resulting electron angle was calculated by a numerical integration of the field without taking into account Larmor rotation. Figures 14 and 15 show typical distributions of the transverse magnetic field and the electron angle along the solenoid, respectively, for $\alpha_0=5\cdot10^{-4}$ rad. Typically, the transverse magnetic field is less than 10 mG and the maximum angle is about $3\cdot10^{-5}$ rad. The latter is in reasonable agreement with the value of $1.3\cdot10^{-5}$ rad given by the formula (22) for the same parameters and $\alpha=\alpha_0=5\cdot10^{-4}$ rad. Linearity of the model results in a linear dependence of the resulting angle on a value of α_0. Therefore, the maximum electron angle is less than $7\cdot10^{-5}$ rad for the value of α_0 up to $1\cdot10^{-3}$ rad.

The restriction on the winding precision can be relaxed further by using dipole correctors so that the integral of the resulting transverse field over the length of every corrector is zero. The maximum angle is anticipated to be somewhere close to centers of correctors and, therefore, can be estimated as $\frac{\theta_{tilt}}{\sqrt{2N_{cor}}}$. To provide the maximum electron angle of below $7\cdot10^{-5}$ rad at N_{cor} = 8, the inclination α_0 should be no more than $4\cdot10^{-3}$ rad which corresponds to the winding precision of ±0.6 mm.

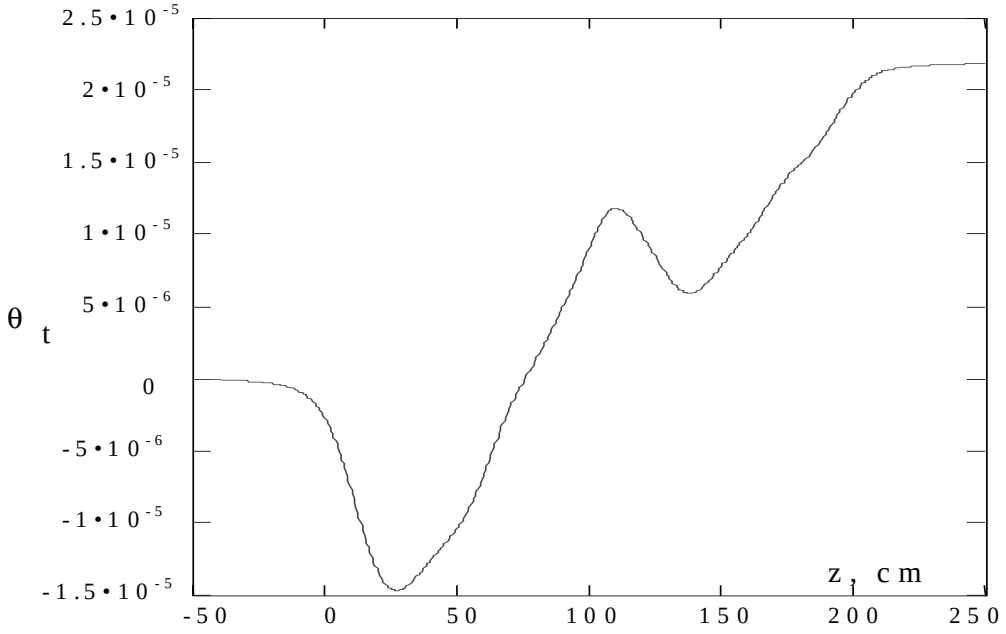

Figure 15: The total angle acquired by an electron in the field shown in Fig.14.

The last winding error we consider is a non-uniformity of the longitudinal coils distribution. If the full number of Ampere-turns in the module is fixed, the resulting angle after passing the entire module is very low (see formula (8)). The resulting azimuthal velocity can be estimated by the formula (10). To keep the electron angle under $7\cdot10^{-5}$ rad, the magnetic field value and the solenoid current density should be homogeneous with the precision of 2.8%.

3.5. Sectioned solenoid module

The rather loose restriction on the longitudinal magnetic field homogeneity (2.8%) makes it possible to design a solenoid module consisting of a number of shorter coils. The coils are placed evenly along the module length, and the average current density is the same as that of a solid module. Possible parameters of such a design are listed in Table 5.

Table 5: Parameters of a sectioned module.

Number of layers	6
Number of turns in one layer	~100
Section length	~20 cm
Wire diameter	2 mm
Current	4 A
Weight of copper	14 kg
Gap size	5 mm
Power	25 W

The gaps between coils have to be small enough to avoid inducing azimuthal velocities. Computer simulations analogous to those made in Section 2 were performed for the design. With the restriction of $7 \cdot 10^{-5}$ rad for the electron angle, the gap size can be up to 5 mm, which is sufficient for current leads etc. To compensate for the possible inclination of the coils, each of them needs a pair of dipole correctors.

4. Conclusion

The restrictions for the solenoid field quality are found to be quite different from those for traditional low-energy electron coolers. The fundamental distinction is based on a simple fact that excitation of an electron velocity, transverse to magnetic lines, by a perturbation in a solenoidal field is maximum when the length of the perturbation, L_p, is about the Larmor period, $\lambda = 2\pi \cdot \rho_L = 2\pi \cdot \gamma\beta mc^2/eB_0$. As a rule, a typical L_p value is close to the solenoid diameter.

Having the solenoid diameter of 30- 50 cm and λ~1- 3 cm << L_p, low-energy coolers keep a low beam temperature due to the adiabaticity of the electron motion. In this case, the excitation of transverse electron velocities is suppressed dramatically with the increase of both the magnetic field and the solenoid diameter and decrease of the electron energy. Electrons strictly follow the magnetic field lines so that deviations of their trajectories from straight lines are determined by local values of the transverse components of the magnetic field.

In contrast, the worst case for the Fermilab's cooler, with the solenoid diameter of 15 cm and λ~100- 300 cm >> L_p, is at the maximum value of the longitudinal field. Electron angles are formed by the integral of transverse magnetic field components so

that averaging of them along the axis is essential. Only the mean winding density must be the same in the solenoid to keep the angles below the critical value. The low strength of the magnetic field makes it possible to drastically decrease the size of the wire, which improves the precision of winding and averages out winding errors better because of an increased number of turns.

These distinctions demand a special consideration of the solenoid design and estimations made above. The main specific conclusions are as follows:

1. For proposed solenoid parameters listed in Table 1, the harmful effects of the gap between solenoids can be compensated by two pairs of solenoidal coils or by one pair and a disk-shaped magnetic shield.
2. The excited electron angle remaining after passing the gap is low if the total number of Ampere-turns in the correction coils is equal to the number of Ampere-turns missing from the solenoid because of the gap.
3. The length of the region of ineffective cooling caused by a gap can be made less than 5% of the total solenoid length if the gap length is 10 cm or lower.
4. The magnetic field quality in the homogeneous part of a module is determined mainly by mechanical distortions of the solenoid body and by possible inclinations of individual turns. Using 8 pairs of dipole correctors per 2 m module, we can achieve the desired magnetic field quality with the precision of wire positioning of ± 0.6 mm.
5. The corrector adjustment has to decrease the transverse field integral under every corrector to below 0.3 G·cm to keep the electron angle change less than $2 \cdot 10^{-5}$. With the corrector length of 25 cm, this value of the integral corresponds to about 12 mG of an average transverse field. The necessary precision of transverse field measurements should be lower by several times, or about $3 \cdot 10^{-5}$ of the longitudinal field.
6. The same solenoid quality can be achieved in a sectioned design.
7. The proposed solenoid design looks doable and less expensive than solenoids of low-energy coolers (per unit length).

5. Acknowledgements

The authors acknowledge that some preliminary estimates for the solenoid specifications were performed by Alexey Burov. We are thankful to him and to Valery Lebedev for many useful discussions.

References

[1] "Prospectus for an Electron Cooling System for the Recycler", Fermilab preprint FERMILAB-TM-2061, edited by J.A. MacLachlan, October 1998.

[2] M.Tiunov. Code SAM. User's Guide, 1999.

[3] J.D.Lawson, The Physics of Charged-Particle Beams, 1977.

[4] S. Humphries, Jr., Principles of charged particle acceleration, 1999.